

Numerical modelling of non-isothermal non-equilibrium mass transfer in the subsurface

William J. Ferguson and A. Kaddouri

Sir William Arrol Building, School of the Built Environment, Heriot-Watt University, Edinburgh EH14 4AS,
SCOTLAND, UNITED KINGDOM
e-mail: W.J.Ferguson@hw.ac.uk

SUMMARY

A three-phase flow and contaminant transport mathematical model for a non-isothermal system is developed and is modelled as a system of six fully-coupled non-linear partial differential equations. The coupled flow of water, air, water vapour and heat is assumed to follow the mechanistic approach of Philip and De Vries. Gravity, viscous and capillary forces are included in addition to non-equilibrium mass transfer (volatilisation and dissolution) based on first-order kinetics. The system of governing equations is solved by employing the finite element numerical solution technique where the modified Galerkin weighted residual method is used for the spatial discretisation whilst the generalised mid-point rule is employed for the temporal discretisation. The non-linearities are handled by both the Newton-Raphson algorithm for the flow equations and the iterative Picard method for the transport and energy equations. The numerical model was validated and verified against several isothermal and non-isothermal analytical and 'benchmark' problems. The effect of a surface temperature variation on the non-equilibrium mass transfer process was investigated and has been shown to have a significant impact on the transport of pollutants in the subsurface.

Key words: *non-equilibrium, three-phase flow, non-isothermal, heat transfer, mass transfer, finite element.*

1. INTRODUCTION

The presence of contaminants in the subsurface can cause serious damage to the environment and pose a major risk to human health [1]. Contaminant substances can originate from toxic waste dumps, in addition to leaking underground storage tanks. In order to understand the processes of groundwater contamination, the past two decades have seen the development of several mathematical models for predicting the transport and fate of contaminants. The majority of the numerical codes developed to date consider only isothermal conditions [2-6]. Non-isothermal conditions can, however, be due to several causes, such as seasonal temperature variations, the technique of remediation (e.g. steam flooding, thermal venting), emplaced

radioactive wastes and the decomposition of chemicals in sanitary landfills. Non-isothermal contaminant flow in unsaturated porous media has been investigated by only a few authors [7-11]. These authors investigated the effectiveness of remediation techniques which involved a variation in temperature. The effect of a seasonal variation of temperature on the mass transfer processes of dissolution and volatilisation was not considered.

This paper presents a three-phase flow numerical model incorporating three mass transfer (volatilisation and dissolution) models. Numerical simulations are presented which highlight the importance of accounting for a surface temperature variation in pollutant transport problems involving NAPL volatilisation and dissolution.

2. MASS TRANSFER MODELS IN ENVIRONMENTAL ENGINEERING

The first models that included dissolution and volatilisation of the pollutant were based on the equilibrium mass transfer formulation, in which the rate of change (due to dissolution and volatilisation) is much greater than due to any other cause and that the flow rate is sufficiently low that equilibrium can be achieved. Models based on the equilibrium mass transfer formulation of the dissolution and volatilisation of the pure NAPL phase have been developed [6, 12, 13].

The terms for dissolution and volatilisation Q_d and Q_v can take the following forms respectively [14]:

$$Q_d = \Phi S_w \lambda_{ed} (C_{wi}) \quad (1)$$

$$Q_v = \Phi S_g \lambda_{ev} (C_{gi}) \quad (2)$$

where λ_{ed} and λ_{ev} are the equilibrium and volatilisation rate coefficient, Φ , S_w and S_g denote the porosity, water saturation and gas saturation and C_{wi} and C_{gi} are the concentrations of the NAPL in the water and gas phases respectively.

This equilibrium theory was later generalised to include the mass transfer of the solid, gas and solute phases in addition to the pure NAPL phase [4, 15].

Considering that the equilibrium in mass transfer processes of dissolution and volatilisation is only reached in particular conditions, the non-equilibrium inter-phase mass transfer was introduced [16]. The terms for dissolution and volatilisation, Q_d and Q_v respectively, can be described by a first order rate law as follows:

$$Q_d = \Phi S_w a_d k_d (\bar{C}_{wi} - C_{wi}) = \Phi S_w \lambda_d (\bar{C}_{wi} - C_{wi}) \quad (3)$$

$$Q_v = \Phi S_g a_v k_v (\bar{C}_{gi} - C_{gi}) = \Phi S_g \lambda_v (\bar{C}_{gi} - C_{gi}) \quad (4)$$

where k_d and k_v are the local dissolution and volatilisation rate coefficients, a_d and a_v are the dissolution and volatilisation specific interfacial areas and \bar{C}_{wi} and \bar{C}_{gi} are the equilibrium concentration of the NAPL in the water and gas phases respectively.

For simple geometrical shapes corresponding to a certain interfacial area, the local rate coefficients can be described using correlations of dimensionless numbers borrowed from the chemical engineering literature [17, 18]. The Sherwood number Sh involves the local dissolution (or volatilisation) rate coefficient, while the flow and diffusion processes are expressed by Reynolds Re and Schmidt Sch numbers respectively. These dimensionless parameters are defined as follows:

$$Sh = \frac{k_d d}{D} = \frac{k_v d}{D} \quad (5)$$

$$Re = \frac{d v^0}{\nu} \quad (6)$$

$$Sch = \frac{\nu}{D} \quad (7)$$

in which D , ν and d are the diffusion coefficient of the material being transferred, the dynamic viscosity and the characteristic length respectively. The characteristic length d is dependent on the type of problem [18].

Along these lines, the NAPL "blobs" were idealised as spheres and the transport equation was solved analytically [19]. However, the local dissolution rate coefficient k_d (or k_v) and the interfacial area between the NAPL and water (or between the NAPL and gas) are complex and very difficult to quantify due to the NAPL heterogeneity. Recent developments have shown that the mass transfer processes could be estimated using laboratory NAPL mass transfer results and quantifying the lumped mass transfer rate coefficient λ_d (or λ_v) instead of the local k_d (or k_v). The influence of the interfacial area is accounted for through the introduction of the NAPL volumetric fraction. The new correlations formula, which has the advantage of being directly related to NAPL experiments for calibration, uses the modified Sherwood number Sh' and is defined as:

$$Sh' = \frac{\lambda_d d^2}{D} = \frac{\lambda_v d^2}{d} \quad (8)$$

Table 1 gives some correlations proposed, where θ_{ni} and δ represent the NAPL initial volumetric fraction and the normalised grain size ($\delta = d_{50} (cm) / 0.05 (cm)$, for spheres $\delta = 0.667$) and x and d_p denote the distance into the NAPL and the mean particle diameter respectively.

Table 1 Mass transfer models

Correlation	Author [Ref.]
$Sh' = 12.0 Re^{0.75} \theta_n^{0.6} Sch^{0.5}$	(9) Miller et al., 1990 [38]
$Sh' = 1240 Re^{0.75} \theta_n^{0.6}$	(10) Parker et al., 1990 [39]
$Sh' = 57.7 (Re)^{0.61} d_{50}^{0.64} U_i^{0.41}$	(11) Powers et al., 1992 [28]
$Sh' = 4.13 Re^{0.598} \delta^{0.673} U_i^{0.369} \left(\frac{\theta_n}{\theta_{ni}} \right)^{\beta_i}$	(12) Powers et al., 1994 [37]
$Sh' = 340 Re^{0.71} \theta_n^{0.87} \left(\frac{x}{d_p} \right)^{-0.31}$	(13) Imhoff et al., 1994 [21]
$Sh' = 10^{-2.79} (Re Sc)^{0.62} \delta^{1.82}$	(14) Wilkins et al., 1995 [20]

The experimental results that have led to the correlations, Eqs. (9)-(14), were all based on a one-dimensional column dissolution test of entrapped NAPL at residual saturation. The correlation by

Wilkins et al. [20], Eq. (14), was obtained from data of entrapped NAPL volatilisation in a one-dimensional unsaturated soil column with still NAPL at residual saturation. We will, therefore, assume in all the examples that will be simulated here, that the NAPL pollutant is at the residual saturation.

The application of the non-equilibrium mass transfer formulation to practical problems in isothermal conditions was carried out by Imhoff et al. [21], Thomson et al. [22], Zhu and Sykes [23] and Rathfelder et al. [24].

Despite the fact that major improvements in the simulation of mass transfer processes have been achieved, the effect of the variation of the surface temperature on the mass transfer processes involved in the subsurface systems has not been investigated. Careful observation of the different models shows the dependence of the mass transfer coefficients on the temperature through the Reynolds and Schmidt numbers. It is, therefore, the objective of this paper to investigate the potential effect of a surface temperature variation on the results of problems involving mass transfer.

The proposed model is a general three-phase non-isothermal formulation for simulating contaminant transport and/or remediation techniques, based on the mechanistic approach of Philip and De Vries [25]. The effect of a surface temperature variation on the mass transfer processes, using three mass transfer models, will be investigated.

3. GOVERNING EQUATIONS OF THE NON-ISOTHERMAL THREE-PHASE FLOW SYSTEM

The mathematical model is composed of six conservation equations, i.e. three equations for the three phases, one for energy and two transport equations for the solute and NAPL vapour. The system variables are the three fluid pressures, the soil temperature and the two NAPL concentrations in the fluid and the gas. The solid soil matrix is assumed to be rigid. The pressure formulation adopted within the mathematical model has no expansion of the storage terms with respect to the fluid pressures and is kept as recommended by Celia and Bouloutas [26]. This method ensures that the formulation is mass conservative when the finite element approximation is used in the solution of sharp front problems.

3.1 Mass conservation of the liquid water and water vapour

The conservation of mass for both the liquid water and water vapour is given by:

$$\begin{aligned} \frac{\partial}{\partial t}(\rho_w \phi S_w) + \frac{\partial}{\partial t}(\rho_w \theta_v) = & -\nabla(\rho_w V_w) - \nabla(\rho_w V_v) - \\ & -\nabla(\rho_w V_g) + \phi S_w \lambda_d (\bar{C}_{wi} - C_{wi}) - \\ & -\phi S_g \lambda_H (H_{wg} C_{wi} - C_{gi}) - Q_w \end{aligned} \quad (15)$$

where V_w, V_g, V_v and V_n are the velocities of water, gas, water vapour and NAPL respectively and are defined as:

$$V_\alpha = -K_\alpha (\nabla P_\alpha + \rho_\alpha g \nabla z) \quad (16)$$

where:

$$K_\alpha = \frac{k_{ra} k}{\mu_\alpha} \quad (\alpha = w, g, n) \quad (17)$$

$$\rho_g = \rho_a + \rho_v + \rho_i \quad (18)$$

in which subscripts g, w, a, v and i represent the gas, water, air, water vapour and NAPL vapour phases, $k_{r\alpha}$ is the relative permeability of the α phase and k is the intrinsic permeability of the soil. The dynamic viscosity μ_w of the water phase is temperature dependent and is defined as follows [27]:

$$\mu_w = 0.6612(T - 229.0)^{-1.562} \quad (19)$$

For the gas and NAPL phase, μ_g and μ_n are as follows:

$$\mu_g = 182 \times 10^{-7} e^{0.634 \log T - \frac{45.638}{T} + \frac{380.87}{T^2}} - 3.45 \quad (20)$$

$$\mu_n = 0.6612(T - 229.0)^{-1.562} \quad (21)$$

The mass densities are temperature, pressure and NAPL solute or NAPL vapour concentration dependent.

It has been assumed that Henry's law governs the transfer of organic compounds between the water phase and the gas phase. In addition, first order kinetics dissolution [16] and first order biodegradation are occurring [28].

Although the theory has been found to have some limitations under special cases [29], the usefulness of the theory was established experimentally by both Cassel et al. [30] and De Vries [29]. Assuming that the water vapour and liquid are in equilibrium then the volumetric water content θ_v is given by [31]:

$$\theta_v = \frac{\phi S_g \rho_v}{\rho_w} \quad (22)$$

The vapour density ρ_v can be written as [31, 32]:

$$\rho_v = \rho_o h \quad (23)$$

$$h = \exp \left\{ \frac{P_w - P_g}{\rho_w R_v T} \right\} \quad (24)$$

where ρ_o is the saturated vapour density, h is the relative humidity, R_v is the vapour gas constant ($R_v = 461.5 \text{ J/kgK}$ [33]) and T is the absolute temperature.

The saturated vapour density ρ_o is given by Mayhew and Rogers [33]:

$$\frac{I}{\rho_o} = 194.4 e^{-0.06374(T-273)+0.1634 \times 10^{-3}(T-273)^2} \quad (25)$$

On the basis of Philip and De Vries' theory, Ewen and Thomas [27] and Thomas and King [34] proposed the following expression for the vapour flux:

$$V_v = -\frac{D_{atm} v \phi_a}{\rho_w} \left\{ \rho_o \frac{\partial h}{\partial P_w} \nabla P_w + \rho_o \frac{\partial h}{\partial P_g} \nabla P_g + \frac{(\nabla T)_a}{\nabla T} \left(\rho_o \frac{\partial h}{\partial T} + h\beta \right) \nabla T \right\} \quad (26)$$

3.2 Mass conservation of gas

Applying the principle of mass conservation to the gas phase yields:

$$\frac{\partial}{\partial t} (\phi \rho_g S_g) = -\nabla \{ \rho_g V_g \} + \phi S_g \lambda_v (\bar{C}_{gi} - C_{gi}) + \phi S_g \lambda_{wg} (HC_{wi} - C_{gi}) - \phi S_g \lambda_{b,n}^g - Q_a \quad (27)$$

The terms on the right hand side of the conservation equation, Eq. (27), are the advection, volatilisation, water-gas pollutant exchange, biodegradation and source terms respectively.

3.3 Mass conservation of NAPL

The conservation of mass for the NAPL in the case of a single component contaminant is given by:

$$\frac{\partial}{\partial t} (\phi \rho_n S_n) = -\nabla (\rho_n V_n) - \phi S_w \lambda_d (\bar{C}_{wi} - C_{wi}) - \phi S_g \lambda_v (\bar{C}_{gi} - C_{gi}) - Q_n \quad (28)$$

The second and third terms on the right hand side of Eq. (28) characterise the dissolution and volatilisation processes respectively [16].

3.4 Heat transfer

The conservation of energy for the soil is given by:

$$\frac{\partial \bar{H}}{\partial t} + \nabla Q = -Q_h \quad (29)$$

in which \bar{H} represents the heat content and is expressed as follows:

$$\bar{H} = H(T - T_r) + \phi S_g \rho_v L \quad (30)$$

where the latent heat is denoted by L and H is the heat capacity of the soil which is given by:

$$H = (1-\phi) \rho_s C_{ps} + \phi S_w \rho_w C_{pw} + \phi S_g \rho_v C_{pv} + \phi S_g C_{ga} C_{pa} + \phi S_g C_{gi} C_{pgi} + \phi S_n \rho_n C_{pn} + \phi S_w C_{wi} C_{pwi} \quad (31)$$

The heat flux per area Q is given by:

$$Q = -\lambda \nabla T + (\rho_w V_v + \rho_v V_g) L + (T - T_r) \{ C_{pw} \rho_w V_w + C_{pv} \rho_v V_v + C_{pv} \rho_v V_g + C_{pa} C_{ga} V_g \} + (T - T_r) \{ C_{pi} C_{gi} V_g + C_{pn} \rho_n V_n + C_{pwi} C_{wi} V_w \} \quad (32)$$

Here an instantaneous thermal equilibrium is assumed among the phases.

3.5 NAPL vapour transfer

The mass conservation equation for the NAPL vapour yields:

$$\frac{\partial}{\partial t} (\phi C_{gi} S_g) = \nabla \{ D_{gi} \nabla C_{gi} \} - \nabla \{ C_{gi} V_g \} + \phi S_g \lambda_v (\bar{C}_{gi} - C_{gi}) + \phi S_g \lambda_{wg} (HC_{wi} - C_{gi}) - Q_{cgi} - \phi S_g \lambda_{b,n}^g \quad (33)$$

where D_{gi} is the hydrodynamic dispersion coefficient in gas that includes both the molecular diffusion and mechanical dispersion [15].

3.6 Solute mass transfer

The mass conservation equation for the solute can be written as:

$$\frac{\partial}{\partial t} (\phi C_{wi} S_w) = \nabla \{ D_{wi} \nabla C_{wi} \} - \nabla C_{wi} V_w + \phi S_w \lambda_d (\bar{C}_{wi} - C_{wi}) - \phi S_g \lambda_{wg} (HC_{wi} - C_{gi}) - \lambda_{b,n}^w \phi S_w C_{wi} - Q_{cwi} \quad (34)$$

where D_{wi} is hydrodynamic dispersion-diffusion coefficient in water similar to the one in gas and $\lambda_{b,n}^w$ represents the first order biodegradation decay coefficient of NAPL in water.

4. NUMERICAL SOLUTION PROCEDURE

The governing set of six partial differential equations are derived from the conservation laws, described in the previous sections, by introducing the phase velocity and phase saturation expressions. The spatial discretisation is carried out by using the modified Galerkin weighted residual finite element method with asymmetric weighting functions as an

upwinding scheme [35]. This scheme is mainly efficient in problems in which the dispersive terms are associated with convective terms. It is worth noting that the system variables are the three fluid pressures P_w , P_g and P_n , the temperature T and the vapour and solute NAPL concentrations C_{gi} and C_{wi} respectively. The set of ordinary differential equations obtained after use of Green's theorem is then discretised in time as follows:

- * The first derivative unknowns are discretised using a backward difference scheme;
- * The generalised mid-point θ method is applied to the first order unknowns.

Finally, the governing non-linear equations are solved sequentially in a staggered manner. At any time step, the three flow equations are first solved simultaneously, then the remaining equations, i.e. the energy and the two transport equations, are solved simultaneously following the calculation of the velocity field at the first stage. The non-linearities of the first system are handled using the Newton-Raphson algorithm whilst the iterative Picard method is used at the second stage.

5. NUMERICAL RESULTS

The proposed generalised three-phase flow formulation has been validated against closed form solutions where a variety of problems, constituting a subset of the general formulation, have been simulated. Very good agreements were obtained between this model and the analytical solutions of Carslaw and Jaeger [36] for the case of both one-dimensional and two-dimensional transient heat transfer. Additionally, the analytical results of steady transport in water and gas with and without biodegradation have been very well reproduced. In order to not obscure and lengthen the presentation, the results are not displayed.

The correctness of the general model will be illustrated by presenting the results of two analyses. Firstly, the results of an isothermal flow and transport problem will be presented, and secondly, the mathematical model will be evaluated by simulating a non-isothermal two-dimensional pollutant and transport problem involving mass transfer, along with a sensitivity analysis of the effect of surface temperature and the choice of mass transfer model.

5.1 Example 1: One-dimensional steady state mass transfer problem

This example constitutes a verification of the accuracy of the proposed model to treat isothermal mass transfer. The domain of interest was discretised using 640 equally spaced elements where $\Delta x = 1.0$ m. For a steady state condition and using the dimensionless numbers Peclet number $Pe' (qk/(\phi SD))$,

Damköhler number $Da (\lambda L/q)$, $c_i = \frac{C_{wi}}{C_{wi}}$ and $\xi = x/L$ in which L is the length of contaminated region across which the flow occurs, Eq. (15), without accounting for the presence of water vapour, can be written as follows [37]:

$$\frac{1}{Pe'} \frac{\partial^2 c_i}{\partial \xi^2} - \frac{\partial c_i}{\partial \xi} + Da(1 - c_i) = 0 \quad (35)$$

The analytical solution is given by Carslaw and Jaeger [36]. Figure 1 shows a comparison of this analytical solution with the numerical solution obtained using the numerical model. As can be seen, excellent agreement is obtained assuming the following data: $L=1$, $v=1$ m/s, $\lambda_d=1$ /s and $\phi S=1$.

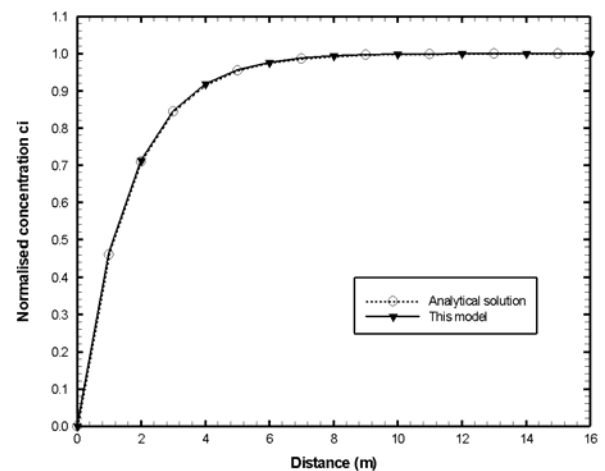


Fig. 1 Numerical and analytical normalised concentration vs. distance

5.2 Example 2: Two-dimensional non-isothermal flow and solute transport

The mathematical model has been used to investigate the effect of a surface temperature variation on the results of a flow and pollutant transport problem incorporating first-order mass transfer kinetics. It is assumed that the NAPL is at the residual saturation. A sensitivity analysis is carried out to investigate the effect of surface temperature and the choice of mass transfer, Eqs. (9) – (14), on the numerical simulation results.

This example concerns the spill of a pollutant into a two-dimensional partially saturated medium at the upper portion of the left-hand boundary, Figure 2. The right hand boundary is maintained at the same initial pressure head value. The pressure head at the upper portion of the left boundary is linear. The domain is 15 cm long and 10 cm deep and is similar to that considered in isothermal analysis without mass transfer by Huyakorn et al. [14]. The domain was discretised using 150 regularly spaced four noded linear quadrilateral elements.

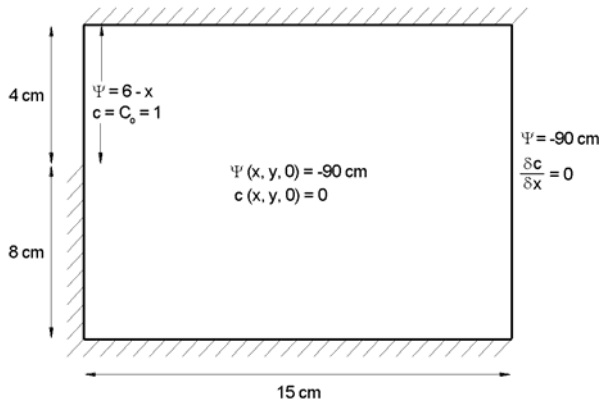


Fig. 2 Two-dimensional flow and pollutant transport geometry

The material properties for the model are presented in Table 2 and the constitutive relationships are as follows:

$$k_{rw} = \frac{S_w - S_{wr}}{I - S_{wr}} \quad (36)$$

$$\frac{\psi - \psi_a}{\psi_r - \psi_a} = \frac{I - S_w}{I - S_{wr}} \quad (37)$$

where $S_{wr} = 0.333$, $\psi_r = -100$ cm, $\psi_a = 0.0$ cm and ψ is the pressure head.

Table 2 Material parameters for the two-dimensional problem (D^* is the coefficient of molecular diffusion and τ is the tortuosity factor)

Material Parameter	Value	Material Parameter	Value
ϕ	0.45	C_{ps}	837 J/kg °C
k	$k=1.1798e-14$	α, β	0.0, 0.0 cm
τD^*	0.01 cm ² /d	λ	0.01 /day
α_L, α_T	1.0 cm, 0.0 cm	λ_T	$0.5+1.15s_w$ W/m °C

Firstly, a series of simulations was carried out to study the effect that a surface temperature variation can have on the flow and transport without mass transfer. Figure 3 shows the horizontal normalised concentration profile for two different surface temperatures, 5°C and 40°C. Figure 3 indicates clearly the significant effect of a surface temperature variation on the transport process, mainly at later time. While an increase in surface temperature with respect to the reference temperature (20°C) has advanced the front, an opposite effect is obtained at a lower temperature. This result is expected since a temperature rise decreases the dynamic viscosity and vice versa.

For mass transfer occurring at constant rate, the results are displayed in Figure 4. The equilibrium condition tends to be approached at later times and at higher temperatures. The normalised concentration at 40°C is found to be up to twice as large as with a surface temperature of 5°C. This ratio is the highest at early times. While the assumption of constant rate mass transfer is interesting in showing the qualitative

importance of non-equilibrium mass transfer, this assumption is not realistic. In the previous section it was demonstrated that all mass transfer models are temperature dependence. The results of the use of the model of Miller et al. [38] are shown in Figure 5 for two different temperatures and it is clearly evident that the rate of mass transfer is dependent on the temperature. A large normalised concentration difference between the two different surface temperatures, which increases with time, is apparent. While at constant rate no difference was observed for locations larger than 5 cm, 7 cm and 13 cm at times 0.053 day, 0.165 day and 0.67 day respectively, Figure 4, the use of a temperature dependent model has given rise to a difference in the results for similar locations and times. For example at later times, the concentration of the temperature dependent model nearly approached the equilibrium state at 40°C and is only 60% of the equilibrium concentration at 5°C, while in the constant rate model, lower concentrations are obtained at 40°C and bigger concentration at 5°C.

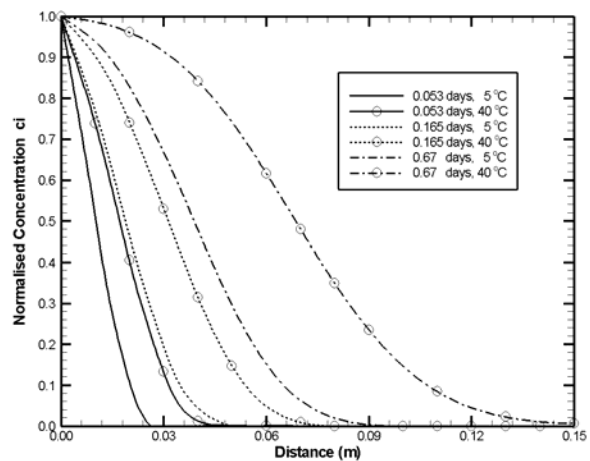


Fig. 3 Computed horizontal normalised concentration at the surface for $T=5^\circ\text{C}$ and $T=40^\circ\text{C}$ (no mass transfer)

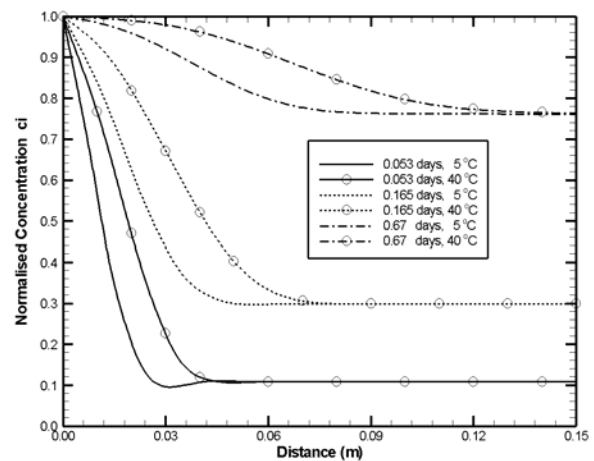


Fig. 4 Computed horizontal normalised concentration at the surface for $T=5^\circ\text{C}$ and $T=40^\circ\text{C}$. Constant $\lambda_d=5.0 \cdot 10^{-5}$ /s

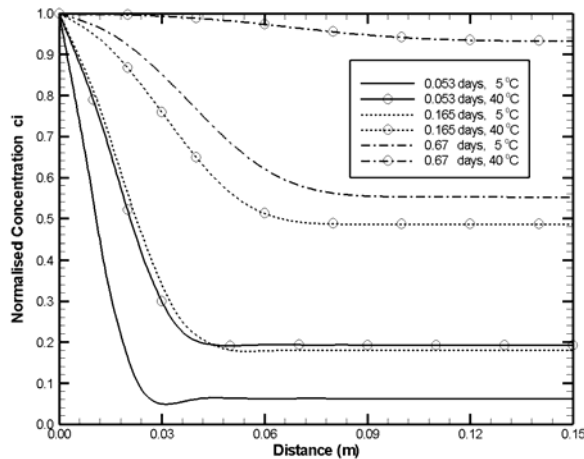


Fig. 5 Computed horizontal normalised concentration at the surface for $T=5^{\circ}\text{C}$ and $T=40^{\circ}\text{C}$ (Dissolution model – Miller et al., 1990)

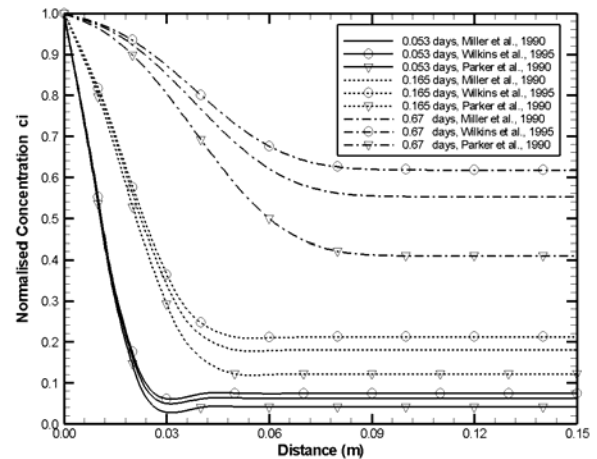


Fig. 6 Influence of the model dissolution on computed horizontal normalised concentration at the surface for $T=5^{\circ}\text{C}$

In order to investigate how the type of model influences the results, the model of Miller et al. [38] was taken as a base analysis. The two other temperature dependent mass transfer models tested were those of Wilkins et al. [20] and Parker et al. [39]. Figures 6 and 7 show the results obtained by the three models at 5°C and 40°C respectively. Firstly, it is worth mentioning the similarity of the response trend of all the three models compared to the constant rate model. Figure 6 shows that although for 5°C the three models are very close early on in the simulation, some differences in the normalised concentration curves arise at later times. The gap between the models increases with time, for a temperature of 5°C , and the numerical solution given by the model of Miller et al. [38] is intermediary with the model of Parker et al. [39] lagging behind. For the temperature of 40°C , larger differences in the results of the three models appear even at earlier times and the model of Miller et al. [38] is still giving the intermediary results with now the model of Wilkins et al. [20] lagging behind. The differences in the behaviour of the models at temperatures greater than the reference temperature of 20°C can be explained by the nature of the expression used by the three models. While the model of Parker et al. [39] does not account for the Schmidt number, the model of Wilkins et al. [20] uses an expression in which the two non-dimensional, Schmidt and Reynolds numbers are raised to the same power. It is worth noting also that the expressions used by the three models are based on different laboratory experiment conditions and materials used. This difference in the response of the models shows the necessity to further explore experimentally the mass transfer mechanism involved. Despite these differences in the models response, it has been shown clearly that the trend in the responses is similar in the three mass transfer models and the surface temperature variation affects significantly the transport of pollutants when mass transfer is considered, and this holds whichever mass transfer model is employed.

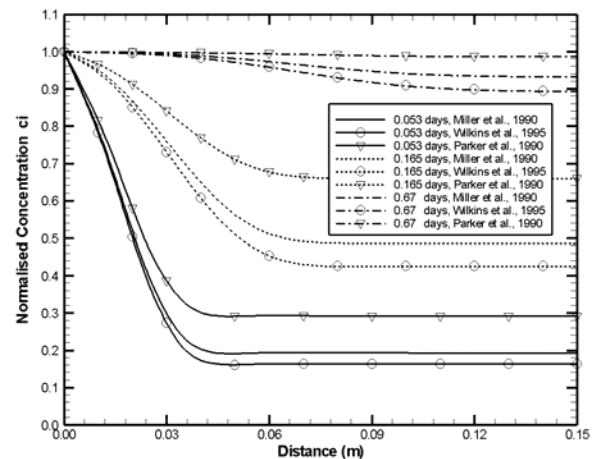


Fig. 7 Influence of the model dissolution on computed horizontal normalised concentration at the surface for $T=40^{\circ}\text{C}$

6. CONCLUSIONS

A theoretical framework has been presented to investigate the potential significance of a surface temperature variation on the transport of pollutants involving mass transfer in subsurface systems. A model describing the three-phase flow and transport of pollutants in non-isothermal porous media has been presented. The coupled flow of water, water vapour, air and heat is assumed to follow the mechanistic approach of Philip and De Vries, which governs the coupled mass and heat transfer. Volatilisation, dissolution and biodegradation are also included.

Verification and validation of the model has been performed on a variety of examples under both isothermal and non-isothermal conditions. The numerical results are shown to be in good agreement with analytical solutions and benchmark problems.

The effect of a surface temperature variation on the non-equilibrium mass transfer process was investigated and was shown to have a significant impact on the transport of pollutants where mass transfer is involved. The results were also found to be influenced by the type of mass transfer model used. It was found that while a constant rate mass transfer gives no difference in the results for locations larger than a certain limit, dependent on time, the use of a temperature dependent mass transfer model has generated differences in the results for similar locations and times. In addition, the trends obtained with the use of three different mass transfer models are all similar in the three variable rate models investigated in comparison to the constant rate model results. It is therefore of paramount importance to account for a ground surface temperature variation in any numerical analysis involving mass transfer.

7. REFERENCES

- [1] R.N. Yong, A.M.O. Mohamed and B.P. Warkentin, *Principles of Contaminant Transport in Soils*, Elsevier, 1992.
- [2] M. Osborne and J. Sykes, Numerical modelling of immiscible organic transport at the Hyde Park landfill, *Water Resour. Res.*, Vol. 22, No. 1, pp. 25-33, 1986.
- [3] C.R. Faust, Transport of immiscible fluids within and below the unsaturated zone: A numerical model, *Water Resour. Res.*, Vol. 21, No. 4, pp. 587-596, 1985.
- [4] A.L. Baehr, Selective transport of hydrocarbons in the unsaturated zone due to aqueous and vapor phase partitioning, *Water Resour. Res.*, Vol. 23, No. 10, pp. 1926-1938, 1987.
- [5] P.S. Huyakorn, S. Panday and Y.S. Yu, A three-dimensional multiphase flow model for assessing NAPL contamination in porous and fractured media, 1. Formulation, *J. Contam. Hydrol.*, Vol. 16, pp. 109-130, 1994.
- [6] L.M. Abriola and G.F. Pinder, A multiphase approach to the modeling of porous media. Contamination by organic compounds. 1. Equation development, *Water Resour. Res.*, Vol. 21, No. 1, pp. 11-18, 1985.
- [7] R.W. Falta, K. Pruess, I. Javandel and P.A. Whitherspoon, Numerical modeling of steam injection for the removal of nonaqueous phase liquids from the subsurface: Part 1. Numerical formulation, *Water Resour. Res.*, Vol. 28, No. 2, pp. 433-449, 1992.
- [8] A.E. Adenekan and T.W. Patzek, Modeling multiphase transport of multicomponent organic contaminants and heat in the subsurface: Numerical model formulation, *Water Resour. Res.*, Vol. 29, No. 11, pp. 3227-3240, 1993.
- [9] P.A. Forsyth, Three-dimensional modelling of steam flush for DNAPL site remediation, *Int. J. Numer. Meth. Fluids*, Vol. 19, pp. 1055-1081, 1994.
- [10] M. Delshad and K. Sepehrnoori, A compositional simulator for modelling surfactant enhanced aquifer remediation, 1. Formulation, *J. Contam. Hydrol.*, Vol. 23, pp. 303-327, 1996.
- [11] H.R. Thomas and W.J. Ferguson, A fully coupled heat and mass transfer model incorporating contaminant gas transfer in an unsaturated porous medium, *Computers and Geotechnics*, Vol. 24, No. 1, pp. 65-87, 1999.
- [12] S. Panday, S. Wu, P.S. Huyakorn, S.C. Wade and Z.A. Saleem, A composite numerical model for assessing subsurface transport of oily wastes and chemical constituents, *J. Contam. Hydrol.*, Vol. 25, pp. 39-62, 1997.
- [13] J.J. Kaluarachchi and J.C. Parker, Modeling multicomponent organic chemical transport in three-fluid-phase porous media, *J. Contam. Hydrol.*, Vol. 5, pp. 349-374, 1990.
- [14] P.S. Huyakorn, J.W. Mercer and D.S. Ward, Finite element matrix and mass balance computational schemes for transport in variably saturated porous media, *Water Resour. Res.*, Vol. 21, No. 3, pp. 346-358, 1985.
- [15] M.Y. Corapcioglu and A.L. Baehr, A compositional multiphase model for groundwater contamination by petroleum products: Part 1. Theoretical considerations, *Water Resour. Res.*, Vol. 23, No. 1, pp. 191-200, 1997.
- [16] B.E. Sleep and J.F. Sykes, Modelling the transport of volatile organics in variably saturated media, *Water Resour. Res.*, Vol. 25, No. 1, pp. 81-92, 1989.
- [17] T.K. Sherwood, R.L. Pigford and C.R. Wilke, *Mass Transfer*, McGraw-Hill, 1975.
- [18] E.L. Cussler, *Diffusion Mass Transfer in Fluid Systems*, 2nd Edition, Cambridge University Press, 1997.
- [19] J.R. Hunt, N. Sittar and K.S. Udell, Nonaqueous phase liquid transport and cleanup - Part I: Analysis of mechanisms, *Water Resour. Res.*, Vol. 24, pp. 1247-1258, 1988.
- [20] M.D. Wilkins, L.M. Abriola and K.D. Pennell, An experimental investigation of rate-limited nonaqueous phase liquid volatilisation in unsaturated porous media: Steady state mass transfer, *Water Resour. Res.*, Vol. 31, No. 9, pp. 2159-2172, 1995.
- [21] P.T. Imhoff, P.R. Jaffe and G.F. Pinder, An experimental study of complete dissolution of a nonaqueous phase liquid in saturated porous media, *Water Resour. Res.*, Vol. 30, No. 2, pp. 307-320, 1994.

- [22] N.R. Thomson, J.F. Sykes and D. Van Vliet, A numerical investigation into factors affecting gas and aqueous phase plumes in the subsurface, *J. Contam. Hydrol.*, Vol. 28, pp. 39-70, 1997.
- [23] J. Zhu and J.F. Sykes, The influence of NAPL dissolution characteristics on field-scale contaminant transport in subsurface, *J. Contam. Hydrol.*, Vol. 41, pp. 133-154, 2000.
- [24] K.M. Rathfelder, J.R. Lang and L.M. Abriola, A numerical model (MISER) for the simulation of coupled physical, chemical and biological processes in soil vapor extraction and bioventing, *J. Contam. Hydrol.*, Vol. 43, pp. 239-270, 2000.
- [25] J.R. Philip and D.A. De Vries, Moisture movement in porous materials under temperature gradients, *Trans. Am. Geophys. Union*, Vol. 38, No. 2, pp. 222-232, 1957.
- [26] M.A. Celia and T. Bouloutas, A general mass-conservative numerical solution for the unsaturated flow equation, *Water Resour. Res.*, Vol. 26, No. 7, pp. 1494-1496, 1990.
- [27] J. Ewen and H.R. Thomas, Heating unsaturated medium sand, *Geotechnique*, Vol. 39, No. 3, pp. 455-470, 1989.
- [28] S.E. Powers, L.M. Abriola and J.W.W. Weber, An experimental investigation of NAPL dissolution in saturated subsurface systems: Steady state mass transfer rates, *Water Resour. Res.*, Vol. 28, No. 10, pp. 2691-2705, 1992.
- [29] D.A. De Vries, The theory of heat and moisture transfer in porous media revisited, *Int. J. Heat Mass Tran.*, Vol. 30, No. 7, pp. 1343-1350, 1987.
- [30] D.K. Cassel, D.R. Nielsen and J.W. Biggar, Soil-water movement in response to imposed temperature gradients, *Soil Sci. Soc. Am. Proc.*, Vol. 33, pp. 493-500, 1969.
- [31] D.A. De Vries, Simultaneous transfer of heat and moisture in porous media, *Trans. Am. Geophys. Union*, Vol. 3, No. 5, pp. 909-916, 1958.
- [32] N.E. Edlefsen and A.B.C. Anderson, Thermodynamics of soil moisture, *Hilgardia*, Vol. 15, No. 2, pp. 31-298, 1943.
- [33] Y.R. Mayhew and G.F.C. Rogers, *Thermodynamics and Transport Properties of Fluids*, Blackwell, Oxford, 1976.
- [34] H.R. Thomas and D.S. King, Coupled temperature/capillary potential variations in unsaturated soil, *J. Eng. Mech. - ASCE*, Vol. 17, No. 11, pp. 2475-2491, 1991.
- [35] P.S. Huyakorn and K. Nilkuha, Solution of transient transport equation using an upstream finite element scheme, *Appl. Math. Model.*, Vol. 3, pp. 7-17, 1979.
- [36] H.S. Carslaw and J.C. Jaeger, *Conduction of Heat in Solids*, 2nd Edition, Clarendon Press, Oxford, 1959.
- [37] S.E. Powers, L.M. Abriola and J.W.W. Weber, An experimental investigation of nonaqueous phase liquid dissolution in saturated subsurface systems: Transient mass transfer rates, *Water Resour. Res.*, Vol. 30, No. 2, pp. 321-332, 1994.
- [38] C.T. Miller, M. Poirier-McNeill and A.S. Mayer, Dissolution of trapped nonaqueous phase liquids: Mass transfer characteristics, *Water Resour. Res.*, Vol. 26, No. 11, pp. 2783-2796, 1990.
- [39] J.C. Parker, A.K. Katyal and J.J. Kaluarachichi, *Modeling Multiphase Organic Chemical Transport in Soils and Groundwater*, US EPA, Oklahoma, 1990.

NUMERIČKO MODELIRANJE NEIZOTERMALNOG I NERAVNOTEŽNOG PRONOSA MASE U PODZEMLJU

SAŽETAK

U ovom radu opisuje se trofazni tok i matematički model transporta zagađivača za neizotermalni sustav koji se modelira kao sustav od 6 povezanih nelinearnih parcijalnih diferencijalnih jednačbi. Pretpostavlja se da vezani tok vode, zraka, vodene pare i topline slijedi mehanistički pristup Philip-a i DeVries-a. Osim neravnotežnog pronosa mase (voltalizacija i otapanje) uključene su gravitacijske, viskozne i kapilarne sile zasnovane na kinetici prvog reda. Sustavi jednačbi su riješeni numerički, metodom konačnih elemenata, primjenom modificirane Galerkin-ove metode za prostornu diskretizaciju, dok je opće trapezno pravilo primijenjeno za vremensku diskretizaciju. Nelinearne jednačbe toka rješavaju se Newton-Raphson-ovim algoritmom, dok se za rješavanje nelinearnih jednačbi prijenosa i energije koristi iterativna Picard-ova metoda. Numerički model je potvrđen i dokazan za nekoliko izotermalnih i neizotermalnih analitičkih i testnih problema. Ispitivao se utjecaj djelovanje promjena površinskih temperatura na proces neravnotežnog pronosa mase te je pokazano da to ima značajan utjecaj na transport zagađivača u podzemlju.

Ključne riječi: neuravnoteženost, trofazni tok, neizotermalni, prijenos topline, pronos mase, konačni element.